Reliability and sensitivity analysis of pultruded GFRP I-sections resistance to flexural and lateral-torsional buckling

Felchak L. W.[1], Machado R. D.[2], Kroetz H.[2]

[1]*Postgraduate Program in Civil Engineering, Federal University of Paraná (UFPR)*
leonardo.wendler@ufpr.br
[2]*Dept. of Civil Structures, Federal University of Paraná (UFPR)*
Polytechnic Center of UFPR, PO Box 19.011, CEP: 81531–980, Curitiba - PR, Brazil
rdm@ufpr.br, henrique.kroetz@ufpr.br

Abstract. Civil industry demands increasingly for materials with outstanding properties and economic viability. In this sense, Pultruded Fiber-Reinforced Polymers (FRP) profiles are experiencing great acceptability and usage in civil construction as innovative structural elements. This is due to its lightness, excellent mechanical properties-to-weight ratios, cost-effective manufacturing process, improved durability and so many other advantages. However, despite the growing application of these materials, there are scarce efforts towards development of recommendations or design standards for FRP structures based on reliability concepts. Frequently in the design of FRP frames buckling phenomena governs the structural ultimate limit state design research, because of the high strength to stiffness ratio of this material compared to conventional ones. The present work evaluates a reliability and sensitivity analysis of global buckling ultimate limit state of I-section pultruded beams, aiming to capture the effect of uncertainties related to non-uniform fiber-resin distribution and loading in the structure reliability index, and its sensitivity to modeled uncertainties.

Keywords: Pultruded GFRP structures; Reliability analysis; Sensitivity analysis.

1 Introduction

In recent decades, fiber-reinforced polymer structural elements (FRP) have gained prominence as a viable and attractive alternative to traditional construction materials. The extensive use of FRP composites in applications involving civil engineering and infrastructure is due to their promising properties, such as a high strength-to-weight ratio, durability, resistance to corrosion, and fatigue (Kaw [1]). Among these applications, glass fiber-reinforced polymer pultruded profiles (GFRP) have been gaining recognition in the construction industry.

The widespread use of fiber-reinforced composite materials in various industries has led to the development of several standards and recommendations to define design procedures and standardizations (Clarke [2], Council et al. [3] and Ascione et al. [4]). However, there are gaps in the design guidelines and literature concerning the behavior of these profiles undergoing buckling, a failure phenomenon that tends to control ultimate limit state anlysis design of pultruded profiles. Due to their high strength-to-stiffness ratio and significant relevance of modulus of elasticity and shear modulus in overall structural safety, GRFP are more prone to local and global buckling than other conventional materials.

Except for the American standard ASCE [5] and a few supplier recommendations (Sørensen [6]), the mentioned standards and procedures do not rely on reliability concepts, raising questions about structural safety and risk management.

Due to the inherent variability in the manufacturing and assembly processes of PRF composite structures, consequently leading to significant sources of uncertainty related to mechanical properties, geometric parameters, loading conditions, imperfections, and mathematical modeling, it is essential to analyze structural performance using a probabilistic approach to properly asses the structure safety.

Incorporating these uncertainties into the ultimate limit state analysis of buckling in pultruded PRF profiles offers a robust approach, providing better understanding of structural safety and risk compared to standard procedures, which could lead to a greater market acceptance and usage of the material.

Many theoretical methods were been proposed to analyze the structural behavior of GFRP composite profiles, mainly based on the assumption that the resin and fiber are uniformly distributed across the profile section, also

known as transverse-isotropic nature at material cross-sections (Qiao and Shan [7], Qiao and Chen [8] and Mottram [9]).

The pultrusion manufacturing process induces unique effects in the final products, such as the introduction of initial imperfections (Bai and Keller [10]), microcracks and non-uniform fiber and resin distributions. Feng et al. [11] highlight the inhomogeneity of the distribution of fibers and resins, and the formation of microcracks in the cross-section of the profiles induced by the manufacturing process itself.

The imperfection generated by non-uniform distribution leads to the manifestation of resin-rich zones and fiber-rich zones. It is known that the percentage of fibers in FRP composites is closely linked to the overall mechanical properties, so the non-uniform distribution of these components results in variable mechanical properties along the cross-section of the profile, such as strength and elastic properties in both the longitudinal and transverse directions, which must be properly considered in structural design and analysis (Nguyen et al. [12], Antin et al. [13] and Ascione [14]).

In this paper two probabilistic models are compared, the first one assessed the probability of failure of an pGFRP FEM model with fiber-resin uniformity across the profile section, while the second one incorporated fiber-resin uncertainties in discrete points and its non-uniform distribution.

Results show

2 Data acquisition of resin content distribution

The database related to experimental measurements of resin content, as well as the geometric parameters of the I sections analyzed, and also the methodology for deriving the mechanical properties were based on Feng et al. [11] article. In this study, the resin content was selected as the criterion for measuring the material uniformity of the pPRFV profiles. Feng et al. [11] use resin content as a parameter to quantitatively describe the non-uniform distribution of fibers and resins because it is easy to measure and because of its relationship with fiber volume, which can be used directly to calculate the material's mechanical properties.

A total of 6 I-sections were subjected to a calcination test procedure to evaluate their resin content. For more details about the geometries and types of resins used in the profiles the reader is invited to see Feng et al. [11] study. In Table 1[1] only the geometry of sample 6 section is shown, which was the unique sample analyzed so far.

Table 1. pPRFV profile geometry

Profile section	Sample	d (mm)	b_f (mm)	t (mm)	Resin type
I-section d x b_f x t	6	200	100	9.5	Epoxy

Source: Adapted from Feng et al. [11].

The sampling locations were selected in such a way that it encompassed all the layers of the composite and was representative of them. For the I sections, samples were taken from nine locations, including three in the flange (with equal spacing), two at the joints between the web and the flange, and four at the midpoints of the top and bottom flanges. The results obtained by Feng et al. [11] for resin content are presented in Table 2, where the average resin content values from three repeated tests are shown. Also shown is the average and the COV (coefficient of variation) which was calculated based on all the sampling points along the cross-section.

[1] d: height, b_f: flange width and t: web and flange thickness

Table 2. Resin contents of I-section

Sample	Resin content (%)									
	Top flange			Web			Bottom flange			Mean (COV)
	TF-1	TF-M	TF-2	W-1	W-2	W-3	BF-1	BF-M	BF-2	
1	20.25	21.60	20.28	20.22	20.36	19.89	20.04	21.74	20.96	20.59 (0.03)
2	23.96	28.80	23.23	32.42	33.74	33.43	22.15	27.65	23.39	27.64 (0.16)
3	23.99	27.00	23.78	29.28	29.29	30.00	25.56	27.54	25.64	26.90 (0.08)
4	25.66	27.75	21.55	33.70	33.99	31.90	28.68	30.05	28.82	29.12 (0.13)
5	30.52	33.06	30.07	29.92	30.16	30.72	26.81	25.05	31.72	29.78 (0.08)
6	26.07	27.44	27.77	30.28	30.16	29.75	20.76	24.72	21.93	26.54 (0.12)

Source: Adapted from Feng et al. [11].

3 Mechanical properties prediction

In this work, the resin content parameter is used as the basis for determining the engineering constants and other mechanical properties for the materials. This methodology was used in the work of Feng et al. [11], and complies with most existing design standards. Possible variations in material properties in the longitudinal direction will be neglected.

In order to apply the classic equations for the mechanical properties of FRP materials, it is first necessary to convert the resin content by weight into fiber volume, according to the following equation:

$$V_{\mathrm{f}} = \frac{(1 - M_{\mathrm{m}})\,\rho_{\mathrm{m}}}{M_{\mathrm{m}}\rho_{\mathrm{f}} + (1 - M_{\mathrm{m}})\,\rho_{\mathrm{m}}} \tag{1}$$

where ρ_{m} is the resin density; ρ_{f} is the fiber density.

The longitudinal elastic modulus E_1 and the major Poisson's ratio ν_{12} calculation are done by the expression:

$$E_1 = E_f V_f + E_m\,(1 - V_f) \tag{2}$$

$$\nu_{12} = \nu_f V_f + \nu_m\,(1 - V_f) \tag{3}$$

where E_f is the longitudinal elastic modulus of the fiber; E_m is the longitudinal elastic modulus of the matrix (resin); ν_f is the Poisson's ratio of the fiber and ν_m is the Poisson's ratio of the resin.

The transversal elastic modulus E_2 e and the shear modulus G_{12} were evaluated by Huang [15] model:

$$E_2 = \frac{E_{\mathrm{f}} E_{\mathrm{m}}\,[V_{\mathrm{f}} + \eta_2\,(1 - V_{\mathrm{f}})]}{E_{\mathrm{m}} V_{\mathrm{f}} + E_{\mathrm{f}}\eta_2\,(1 - V_{\mathrm{f}})} \tag{4}$$

$$\eta_2 = \frac{0,2}{1 - \nu_{\mathrm{m}}}\left(1,1 - \sqrt{\frac{E_{\mathrm{m}}}{E_{\mathrm{f}}}} + \frac{3,5E_{\mathrm{m}}}{E_{\mathrm{f}}}\right)(1 + 0,22V_{\mathrm{f}}) \tag{5}$$

$$G_{12} = \frac{G_{\mathrm{f}} G_{\mathrm{m}}\,[V_{\mathrm{f}} + \eta_{12}\,(1 - V_{\mathrm{f}})]}{G_{\mathrm{m}} V_{\mathrm{f}} + G_{\mathrm{f}}\eta_{12}\,(1 - V_{\mathrm{f}})} \tag{6}$$

$$\eta_{12} = 0,28 + \sqrt{\frac{E_m}{E_f}} \tag{7}$$

$$\nu_{21} = \nu_{12}\frac{E_2}{E_1} \tag{8}$$

where G_f is the shear modulus of the fiber; G_m is the shear modulus of the matrix (resin); η_2 and η_{12} are coefficients utilized in the calculation of E_2 e G_{12}, respectively; and ν_{21} is the minor Poisson's ratio.

The mechanical properties of the fiber and resins considered in analysis are provided in the following table:

Table 3. Mechanical properties of fiber and resins

Material	Property	Symbol	Value
Fiber	Density (kg/m^3)	ρ_f	2600
	Young's Elastic Modulus (GPa)	E_f	81
	Shear Elastic Modulus (GPa)	G_f	33
	Poisson's Ratio	v_f	0.22
Epoxy Resin	Density (kg/m³)	ρ_m	1300
	Young's Elastic Modulus (GPa)	E_m	3.7
	Shear Elastic Modulus (GPa)	G_m	1.4
	Poisson's Ratio	ν_m	0.35

Source: Adapted from Feng et al. [11].

4 Finite element modeling

Finite element modeling (FEM) was conducted to evaluate the critical buckling load of the structure. For this purpose an eigenvalue buckling analysis was built via ANSYS (Ansys [16]). Until now, only results related to I-section 200 × 100 × 9.5 mm were obtained so on. The measured resin contents were specified in the model, a slenderness ratio of 200 was chosen to ensure global ocurrence of global buckling modes. Field variables built-in functions of ANSYS (Ansys [16]) were used to define the pGFRP as a field variable depended orthotropic elastic material, in order to consider mechanical properties variation across the section profile. The field variable was specified as the measured resin contents, and tabular data was provided to define relationships between the field variable and orthotropic elastic material properties. As mentioned in previous section it was assumed that the resin content variations of a section remained constant throughout the length of the pGRFP beam.

The I-section profile model is shown in Figure 1 with respective boundary conditions. The beam is 4m long (ensuring a slenderness ratio nearly 200 in minor axis), SHELL281 elements were used with a of 8mm size and aspect ratio of 1:1, a mesh judged very acceptable after some convergence tests. The two end sections edge are fixed (translations and rotations in all directions were set equal to zero) and a uniform distributed line load is applied at the beam top flange. The load applied and the resin content at sampling points were modeled as random variables as will be discussed in the further section.

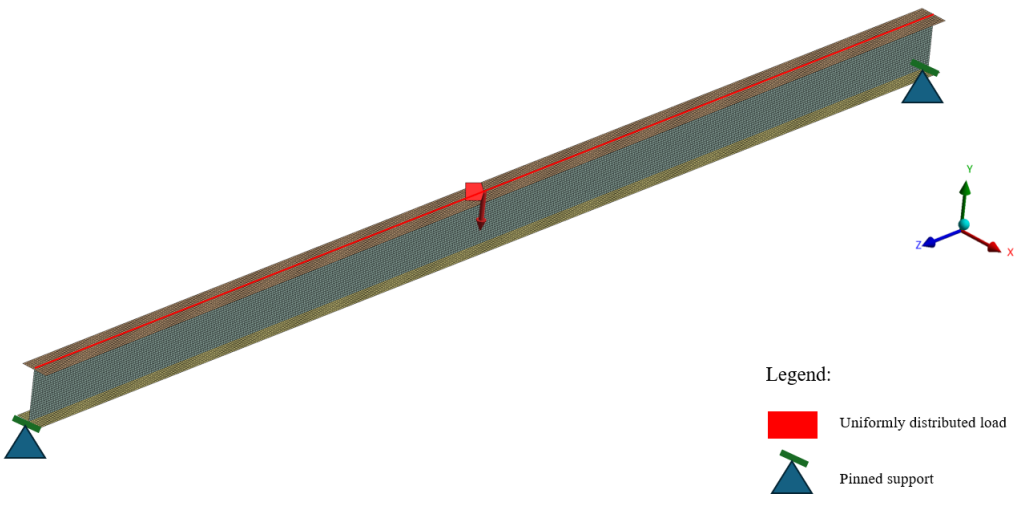

Figure 1. Finite element model

5 Reliability problem

Two distinct realibility problems are proposed and compared to study the sample 6 results. The first one comprehends modeling the pGFRP profile considering a uniform distribution of the fiber-resin content, given as the mean of the sample 6 measured resin contents. The second involved a structural reliability analysis considering the variability of the resin content at every sampling point as a uniform random variable, which ranges from the minimum to the maximum measured values at every sampling point.

The limit state function is defined as follows:

$$g\left(\mathbf{X}\right) = \lambda_{i,crit} - 1 \leq 0 \tag{9}$$

where $\lambda_{i,crit}$ is the first eigenvalue, or load multiplier of the applied load, which leads to the first critical buckling load of the structure. The corresponding probabilistic model consists of the 10 independent random variables defined in Table 4:

Table 4. Probabilistic model parameters

Random variable	Distribution	Parameter	CoV (%)
q (N)	Normal	15000 (mean)	10
RC TF-1 (%)	Uniform	20.25-30.52 (range)	-
RC TF-M (%)	Uniform	21.60-33.06 (range)	-
RC TF-2 (%)	Uniform	20.28-30.07 (range)	-
RC W-1 (%)	Uniform	20.22-33.7 (range)	-
RC W-2 (%)	Uniform	20.36-33.99 (range)	-
RC W-3 (%)	Uniform	19.89-33.43 (range)	-
RC BF-1 (%)	Uniform	20.04-28.68 (range)	-
RC BF-M (%)	Uniform	21.74-30.05 (range)	-
RC BF-2 (%)	Uniform	20.96-31.72 (range)	-

First order reliability method (FORM) algorithm with iHLRF search scheme for MPP (most probable point ou design point) was implemented in Python language. While executing the algorithm the FEM model needs to be evaluated at each iteration, in order to compute $g\left(\mathbf{X}\right)$ and it's gradient vector. As the function given by eq. 9 has no analytical expression, the gradient is unknown and needs to be computed using numerical techniques. So a forward finite difference scheme was employed to calculate the components of the limit state function gradient vector. FORM was initialized with the random variables mean values, the optimal step calculation for MPP (most probable point in standard normal space) evaluation was done by Armijo rule.

6 Results and discussion

The FORM results for the both conditions of analysis are presented in Table 5.

Table 5. FORM analysis results

Output	Model	
	Fiber-resin uniformity	Fiber-resin non-uniformity
p_f	9.261E-05	3.018E-04
β	3.738	3.430
Model calls	10	108

Table 5 shows preliminarly results for the proposed analysis, a higher probability of failure can be observed when the fiber-resin non-uniformity is considered, consequently leading to a minor relibility index β. Also the incorporation of the mechanical properties variability demanded a higher computational cost, increasing the number of model calls necessary for convergence.

Figure 2 presents the local sensitivity indexes, i.e. importance factors obtained in FORM analysis. The load shows higher importance, since it have a direct and explicit effect in the eigenvalues scale, and consequently on the limit state function values as stated by Equation 9. The sensibilities related to the resin content are aproximately similar, except for RC W-1 variable, which is located at the top part of the beam web. So it is possible to infer that resin content variation at any sampling poing results in a similar resistance change.

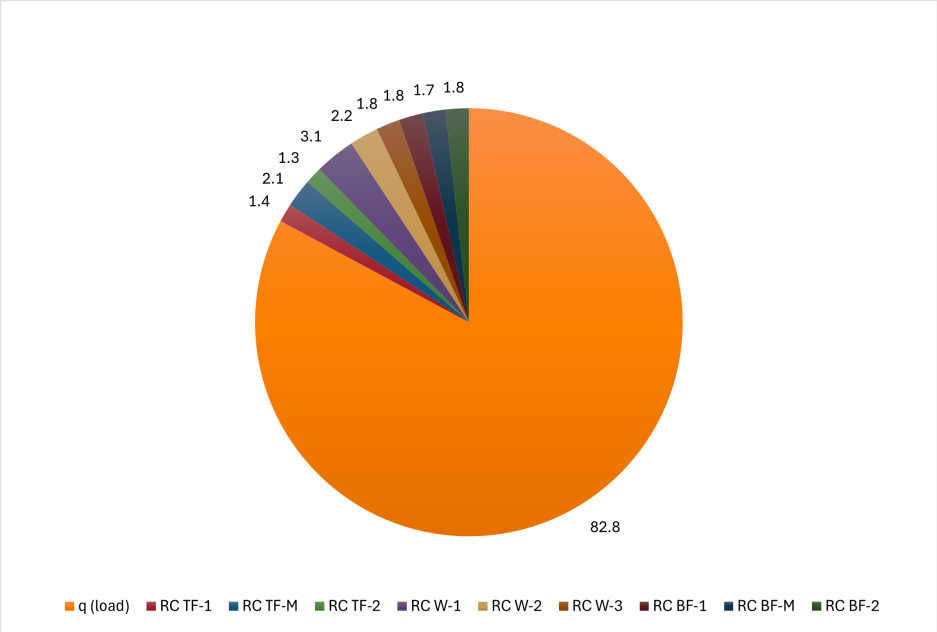

Figure 2. FORM analysis importance factors

7 Conclusions

Based on the results of the numerical simulations and their comparison, the following conclusions can be summarized:

1. Non-uniform fiber-resin distribution is a type of inherent initial imperfection in pGFRP, which may reduce global buckling resistance, and the member reliability related to that structural mode of failure;
2. FEM is built to analyze the influence of non-uniform material on compressive member, a parametric model is set up at ANSYS enabling the implementation of iterative schemes. FORM algorithm preliminarly results show that fiber-resin uniformity assumption increased the overall section resistance to global buckling, leading to higher realibility index when compared to profiles with non-uniform fiber-resin distribution.

Acknowledgements. The authors thank Federal University of Paraná, National Council for Scientific and Technological Development (Conselho Nacional de Desenvolvimento Científico e Tecnológico (CNPQ)), and Coordination for the Improvement of Higher Education Personnel (Coordenação de Aperfeiçoamento de Pessoal de Nível Superior (CAPES)) for the financial support and infrastructure.

Authorship statement. The authors hereby confirm that they are the sole liable persons responsible for the authorship of this work, and that all material that has been herein included as part of the present paper is either the property (and authorship) of the authors, or has the permission of the owners to be included here.

References

[1] A. K. Kaw. *Mechanics of composite materials*. CRC press, 2005.

[2] J. L. Clarke. *Structural design of polymer composites: Eurocomp design code and background document*. CRC Press, 2003.
[3] N. R. Council and others. Guide for the design and construction of structures made of frp pultruded elements. *CNR-DT*, vol. 205, pp. 25–31, 2007.
[4] L. Ascione, J.-F. Caron, P. Godonou, van K. IJselmuijden, J. Knippers, T. Mottram, M. Oppe, M. G. Sorensen, J. Taby, L. Tromp, and others. Prospect for new guidance in the design of frp. *Ispra: EC Joint Research Centre*, 2016.
[5] ASCE. *Load and Resistance Factor Design (LRFD) for Pultruded Fiber Reinforced Polymer (FRP) Structures*. American Society of Civil Engineers, 2024.
[6] J. Sørensen. Design of fibre reinforced polymer structures–load combinations and partial factors to be used together with jrc document on 'design of frp'-with fiberline products, 2016.
[7] P. Qiao and L. Shan. Explicit local buckling analysis and design of fiber–reinforced plastic composite structural shapes. *Composite Structures*, vol. 70, n. 4, pp. 468–483, 2005.
[8] P. Qiao and Q. Chen. Post-local-buckling of fiber-reinforced plastic composite structural shapes using discrete plate analysis. *Thin-Walled Structures*, vol. 84, pp. 68–77, 2014.
[9] J. Mottram. Lateral-torsional buckling of thin-walled composite i-beams by the finite difference method. *Composites Engineering*, vol. 2, n. 2, pp. 91–104, 1992.
[10] Y. Bai and T. Keller. Shear failure of pultruded fiber-reinforced polymer composites under axial compression. *Journal of Composites for Construction*, vol. 13, n. 3, pp. 234 – 242, 2009.
[11] P. Feng, Y. Wu, and T. Liu. Non-uniform fiber-resin distributions of pultruded gfrp profiles. *Composites Part B: Engineering*, vol. 231, pp. 109543, 2022.
[12] T. Nguyen, T. Chan, and J. Mottram. Influence of boundary conditions and geometric imperfections on lateral–torsional buckling resistance of a pultruded frp i-beam by fea. *Composite Structures*, vol. 100, pp. 233–242, 2013.
[13] K.-N. Antin, A. Laukkanen, T. Andersson, D. Smyl, and P. Vilaça. A multiscale modelling approach for estimating the effect of defects in unidirectional carbon fiber reinforced polymer composites. *Materials*, vol. 12, n. 12, 2019.
[14] F. Ascione. Influence of initial geometric imperfections in the lateral buckling problem of thin walled pultruded gfrp i-profiles. *Composite Structures*, vol. 112, pp. 85–99, 2014.
[15] Z. M. Huang. Micromechanical strength formulae of unidirectional composites. *Materials Letters*, vol. 40, n. 4, pp. 164–169, 1999.
[16] Ansys. *Ansys 2024 R1 Release Documentation, Theory and Modelling Guide*. ANSYS, Inc. Canonsburg, PA, 2024.